Method of Rapid Mix EPR Applied to the Folding of Bi−Spin-Labeled Protein as a Probe for the Dynamic Onset of Interaction between Sequentially Distant Side Chains†

Vladimir M. Grigoryants, Kim A. DeWeerd, and Charles P. Scholes*

Department of Chemistry, Center for Biophysics and Biochemistry, University at Albany, SUNY, Albany, New York 12222

Received: July 29, 2003; In Final Form: December 19, 2003

The time scale over which an interaction between distant residues is established impacts the nature of protein folding. Our method for probing the interaction between distant residues is the result of newly developed rapid-mix flow EPR apparatus and of cysteine-directed spin labeling. In our method, entire spectra of bi-labeled protein have been acquired with better than millisecond time resolution after the start of folding. To do this, we use an ultra rapid ball-mixer interfaced to a mini dielectric resonator and combined with simultaneous rapid field scanning. Details of the specialized mixer, resonant structure, and the field sweep/data gathering are presented. This initial application focused on iso-1-cytochrome *c* cysteine-specifically bi-labeled at the cysteine-mutated sites, Ser47Cys and Lys79Cys. These are sequentially distant sites whose unmutated side chains in folded protein are less than 10 Å away from each other and whose spin labels are ∼14 Å distant as evidenced by spin−spin dipolar broadening of the EPR spectrum from the folded bi-labeled protein. During flow, we observed entire EPR spectra of folding protein with ages of 380 μs and 1.2 ms, referenced to the start of folding. Absence of dipolar-broadening showed that folding had not sufficiently proceeded at 380 microseconds or 1.2 milliseconds to cause the sequentially distant spin labeled side chains of residues 47 and 79 to achieve the conformation they have in folded protein, although diminishment of the EPR peak intensities was consistent with local probe enfolding/immobilization. Spectra obtained with rapid field scans triggered 1 s after the start of folding in the stopped-flow EPR mode showed significant, albeit incomplete, onset of the dipolar broadening interaction between the labels on Ser47Cys and Lys79Cys.

Introduction

A major objective of modern structural biology is to understand the structure, dynamics, and conformations of biomolecules as they fold into or unfold from their three-dimensional, biologically active structures. Achieving this objective means following and understanding the structure and evolution of partially folded intermediates, delineating local versus global events, and obtaining evidence for establishment of contacts between sequentially distant, folding macromolecular components. Our previous methods of rapid-mix flow and stopped-flow EPR (electron paramagnetic resonance) at a single field with single site-directed spin labeling have already provided a distinctive view of protein folding[1] extending into the submillisecond regime at sites not previously studied by other techniques.[2,3] We extend out methods by rapid field scanning and cysteine-directed bi-labeling to probe for establishment of tertiary interaction between amino acid side chains that are far apart in sequence but close to each other in final folded form.

Overview of Cytochrome Folding. Our initial choice for study is the heme protein iso-1-cytochrome *c* (iso-1-cyt *c*) whose ribbon diagram is shown in Figure 1. Within the limitation of rapid-mixing techniques having dead times longer than a millisecond, the folding of cytochromes was historically followed from optical changes at the heme which reported heme liganding change, from tryptophan fluorescence quenching which reported overall decrease in the heme-iron-to-Trp59 distance[4,5] and from hydrogen/deuterium (H/D) exchange which reported folding-induced stabilization of hydrogen bonds.[6] The resultant folding kinetics[6,7] showed a fast phase in the 5−100 ms range, thought to represent the critical rate-determining step of cytochrome folding, a step requiring significant activation energy in which polar and nonpolar groups were buried in a concerted fashion. There was a slower 0.5−1 s phase unique to cytochrome which was required for states trapped with improper heme-histidine mis-ligation to recover their proper heme-Met80 ligation.[8,9]

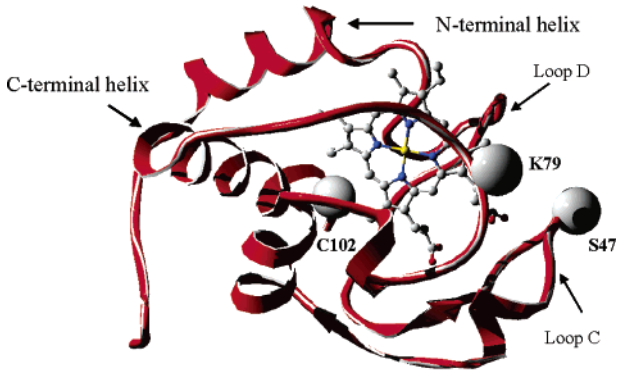

Figure 1. Ribbon diagram of iso-1-cyt-c showing the nearby pair of double mutation sites, Ser47 (S47) and Lys79 (K79)for kinetic study: S47 and K79 lie close in the folded protein (side chains <10 Å distant) but 32 residues away in sequence. Also shown are the heme and Cys102, which was the initial and naturally occurring cysteine labeling site. Coordinates for the diagram were taken from the PDB data of ref 32.

There were also changes occurring within less than the millisecond dead time of a standard mixer, too early explicitly to be measured. What was called a "burst" stage (occurring in less than 5 ms after the start of folding) was suggested to be formation of a compact state with incompletely defined helical

† Part of the special issue "Jack H. Freed Festschrift".

* To whom correspondence should be addressed. Phone: 518-442-4551. Fax: 518-442-3462. E-mail: cps14@albany.edu.

10.1021/jp030925b CCC: $27.50
Published on Web 03/20/2004

structure.[7,10,11] Following technical development of ultrafast mixers and laser-triggered methods, evidence on the submillisecond level was obtained for general protein compacting from CD (circular dichroism),[12] from small-angle X-ray scattering,[13] and from heme-driven fluorescence quenching.[14,15] In addition, there was evidence for a heme ligation change.[16−19] Except at the heme, the time scale and location of prefolding were at best indirectly inferred. The requirements now for better understanding of submillisecond events are not just techniques to show that they happen, but experiments to show where they happen. With experiments extending into the submillisecond range on selected singly and doubly labeled systems, we are in the process of elucidating where and how prefolding happens.

Previous Flow and Stopped-Flow EPR of Folding Spin Labeled Iso-1-cyt *c*. Dielectric resonator-based EPR preceded by closely integrated rapid-mixing was our starting point for ambient temperature stopped-flow and flow EPR. The technique started with a grid mixer[20] and has progressed to a much more rapid ball-mixer for which the details of calibration of dead time, sample age, and mixer efficiency are set out in refs 2 and 21. Flow and stopped-flow EPR provided a new way of following nanosecond molecular tumbling motions of methanethiosulfonate spin label (MTSSL) specifically attached at cysteine[22−24] as those motions were themselves modulated by protein folding on the submillisecond and longer time scale. Our initial kinetic EPR study on iso-1-cyt *c* was done at its naturally occurring Cys102.[1] Subsequently, we systematically probed protein folding at separate mutation-tolerant, externally located cysteine labeling mutation sites as follows: Thr8Cys, Glu66Cys, and Asp92Cys, which are in helices, and Glu21Cys, Val28Cys, His39Cys, Asp50Cys, and Lys79Cys, which were in loops. An *E. coli* expression system was developed to provide 100 mg (overnight) quantities of each cytochrome mutant.[3] Single labels on protein when folded were generally more encumbered by their environment and showed the broader and less intense derivative EPR features that indicated nanosecond or longer tumbling times, whereas the spin labels attached to unfolded protein were generally less encumbered by their local environment and showed narrower, more intense derivative features indicating local subnanosecond tumbling times of the probe. (See the Methods of Analysis and the Supporting Information from ref 1 and the references therein of Miick and Millhauser,[25] Marsh,[26] and Schneider and Freed,[27] for a summary of how EPR line widths of single, protein-attached spin labels increase and derivative peak heights decrease with increasing tumbling correlation times.) The mutated locations studied were not previously directly probed by other techniques, and we observed them on a kinetic time scale stretching from 50 microseconds to seconds. All spin labeled regions of the protein, not just the N and C terminal helical locales identified by hydrogen exchange,[6,8,28] experienced a global phase of folding at pH 5 and room temperature. At pH 5 and at a concentration of exogenous imidazole[29] that eliminated the kinetic trap of heme mis-ligation, this global phase had a 20−30 ms decay time. This global phase was a simple yet important finding for the folding of cytochrome *c*. In the absence of exogenous imidazole at pH 5, there was a major phase of folding whose longer ~1 s recovery time we have attributed to recovery from the kinetic trap of heme-histidine mis-ligation.[29] With or without the exogenous imidazole, there was a burst of rapid EPR signal change that occurred during the several millisecond dead time of the stopped-flow mixer, and investigating the nature of this burst has been a major emphasis which has led to our new EPR methods.

To elucidate the time-development of this burst, a rapid ball-mixer having <0.5 μL dead volume was tightly integrated to the dielectric resonator so that by varying the flow velocity, and consequently, the delivery time of sample from mixing point to the EPR observation zone, the EPR signal intensity of folding protein could be followed to within less than 100 μs after start of folding. There was direct evidence for a burst of folding or protein compacting at spin labeled Cys102 that occurred within 150 μs of mixing at 20 °C and within 500 μs of mixing at 7 °C. By contrast, rapid flow study of the mutant Asp50Cys spin labeled at position 50 in loop C showed probe immobilization on the 50 μs time scale, an order of magnitude faster than Cys102 showed at a comparable temperature.[3]

The previous stopped-flow and continuous-flow EPR were undertaken at a single field.[1−3] The rapid scan magnetic field method presented in this paper provides more information from entire kinetically varying field swept spectra than does the collection of a kinetically varying EPR amplitude at a single field. In previous efforts aimed under equilibrium conditions at T4 lysozyme, entire spectra for either liquid[30] or frozen[31] bi-labeled species have provided information on the dipolar coupling between bi-labels which shows proximity of the labels. T4 lysozyme spectra under ambient liquid conditions showed $1/T_2$ dipolar broadening inversely proportion to the sixth power of the interprobe distance R^{-6} and proportional to the protein tumbling correlation time, τ_c.[30] Building on our experience in kinetic EPR applied to spin labeled iso-1-cyt *c*, we chose to label for this initial bi-label study the side chains of Ser47 (S47) and Lys79 (K79) in Figure 1 which have a 32 residue separation in primary sequence but a close 9 Å separation of β carbons in the crystal.[32] Cysteine-directed spin labeling of the double mutant S47C/K79C afforded the doubly labeled form which we call "S47C−SL/K79C−SL". We thus present a new method to take overall time-resolved spectra, and in the specific case here, we apply it to track the time development of the proximity of spin labeled residues at positions 47 and 79.

Methods and Materials

Standard CW (Continuous Wave) EPR Spectroscopy. Our CW EPR system was a Bruker ER-200 D-SRC X-band spectrometer which was interfaced to a PC equipped with an IBM analog-to-digital converter and Scientific Software Services Systems (Bloomington, IL) EW 2.41A software as described in refs 2 and 3. Standard CW first derivative ($d\chi''/dH$) EPR spectra were obtained with a small, high sensitivity X-band dielectric resonator (DR) using samples of approximately 0.5 μL volume. Microwave power of 1 mWatt (milliwatt) and modulation of ~1 G (Gauss) were chosen so as not to broaden the EPR spectrum.

Equipment for Flow EPR with Rapid Field Scan. We have developed a miniature quartz sample capillary containing a micro (0.4 mm diameter) platinum ball-mixer.[2] The device provided at fastest flow rates a 70−90 μs time resolution between mixing and observation.[3] The overall system was based on a dielectric resonator (DR) with 30-fold greater sensitivity than standard EPR resonators,[21] an EPR active volume of 0.36 μL, and an experimentally measured 0.25 μL volume from the mixing point to the center of the EPR zone. The experimental calibration of the timing scale and dead volume was obtained as previously reported by Grigoryants and co-workers [2] from the kinetics of destruction of TEMPO (2,2,6,6-tetramethyl-4-piperidinol, Sigma) spin probe by high concentrations of sodium dithionite.

To control flow, the model 715 Syringe Ram Controller (Update Instrument, Inc., Madison, WI) was modified to provide

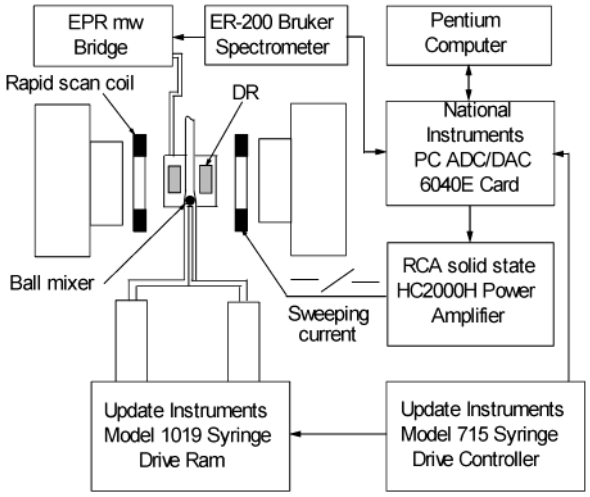

Figure 2. Block diagram of continuous-flow and stopped-flow EPR setup for triggered synchronized rapid field scan.

a wider range of syringe ram velocities from 0.08 cm/s up to 8 cm/s. The original Update syringe ram drivers were also modified with high precision linear bearings from Lempco Industries Inc. (Santa Fe Springs, CA) to prevent dynamic mis-matching of the liquid feed from the syringes. The practical range of flow velocities was restricted by quality of mixing at the lower velocities (e.g., 140 μL/s or 0.5 cm/s) and the breakage tolerance of glass barrels at high velocity (e.g., 2700 μL/s or 8 cm/s). To prevent the latter breakage, heavy duty syringe glass barrels with 30 mm o.d. and 4.6 mm i.d. (Wilmad Glass Co., Buena, NJ) were employed. It was critical to have syringe plungers made of a material which had low friction with the syringe barrel walls and which still maintained their precise plunger size at high pressure and low temperature; the material used for the plungers was Delrin/Teflon rod (MSC Industrial Supply). Our variation of velocity method provided tested delivery times from mixer to the center of the EPR active zone in the range of 0.09 ms to 1.4 ms. The temperature of the EPR resonator assembly, syringes, and input tubes was controlled by a model RTE-9B Refrigerated Circulating Bath (Neslab, Newington, NH) and additional thermistor sensors which were attached to the body of the resonator and to the syringes. The EPR assembly was wrapped with aluminum foil to average the temperature distribution over the whole device and was insulated with plastic film.

Our data acquisition system for rapid magnetic field scan was based on a PC Pentium/166 MHz and ADC/DAC PC Card 6040E from (National Instruments, Austin, TX). This card allowed simultaneous high speed digitization of the EPR analogue signal and creation of an output voltage that directly fed the magnetic field sweep power amplifier. A solid-state DC power amplifier (HC2000H from RCA) provided current for the rapid magnetic field sweeping. The current from the power amplifier was provided via high current connections to two 2Ω Helmholtz coils, each of 90 mm diameter, which were located 20 mm away from the magnet pole faces so that they would not perturb the field-stabilizing Hall sensor. The fast magnetic field sweep we used was stable to less than 0.1 G and linear to within 1.5% over a range of 130 G. Lab View software from National Instruments (Austin, TX) was used to program the rapid, repetitive collection of data with 12-bit resolution during flow and simultaneously to drive the field sweep so that precise, repetitively overlaid spectra could be obtained in synchrony with the linear field sweep.

A schematic of our variable velocity flow system is provided in Figure 2. With our ball-mixer systems, we show here kinetic rapid scans with sample ages 380 μs (microseconds) and 1.2 ms which were obtained under conditions of continuous-flow. A ball-mixer system with an experimentally measured 0.25 μL volume from the mixing point to the center of the EPR zone was utilized for accumulating the most rapid scanned spectra in the 0.1−1.2 ms range (e.g., Figures 4, part A and B below), and with it we obtained a 50:1 signal noise for data collected during several seconds of flow with a modulation field of 1.6 G. This meant that for a sample whose age after mixing was 1 ms we would use approximately 1 mL of about 400 μM reactant ($\sim$ 5 mg of cytochrome).

The spectrum (Figure 4C) with 1 s age after mixing was obtained from 75 rapid scans (50 ms duration) triggered 1 s after stopped-flow at which point in time there remained a slow phase of folding with a $\sim$ 1 s decay time. The method of obtaining spectra by rapid field scans following stopped-flow is inappropriate for signals which are undergoing marked kinetic change during the course of a sweep. In recognition of this problem, we are currently developing a modification to increase the distance between the mixer and the dielectric resonator by 10−30 times so that we can use variable flow EPR with rapid magnetic field sweep to observe samples whose age since mixing is 10−300 ms and whose kinetic decay time is in the 10−300 ms range.

Sample Conditions for Kinetic EPR. Folding for continuous-flow and stopped-flow measurements was routinely induced by mixing protein unfolded in 2 M GdnHCl (guanidinium hydrochloride ultrapure, Sigma) pH 5.0 in a 1:2 fashion with dilute 0.05 M pH 5.0 Na acetate buffer to a 0.66 M GdnHCl concentration where the protein refolded. The GdnHCl concentration where the protein was approximately half folded was approximately 1 M. Initial stopped-flow measurements carried out at the central peak maximum indicated a rapid burst of compacting which diminished the EPR intensity in less than 4 ms. Our work was carried with no exogenous imidazole, and as a result, there was the $\sim$1 s kinetic phase attributed to folding slowed by kinetic trapping from histidine misligation.[3,29] A concern in using exogenous imidazole is that NMR study has shown that exogenous imidazole disrupts the locale of Met80, and this disrupted locale includes Lys79.[33]

CD Spectroscopic Characterization. Circular dichroism (CD) data were collected from iso-1-cyt *c* by use of an Aviv 62DS spectrometer fitted with a thermostated sample changer as previously described.[1,3] CD spectra in the far-UV (ultraviolet) from 210 to 250 nm are an indicator of helical content. The thermal denaturation studies were carried out by monitoring changes in ellipticity with respect to temperature at 222 nm.

Cysteine Mutants of Iso-1-Cyt *c*. A high yield *E. coli* heterologous expression system[34,35] was used to overexpress mutant iso-1-cyt *c*.[3] Site-directed mutagenesis was performed[36−39] as detailed in the Supporting Information of ref 3. Plasmids that were confirmed by DNA sequencing to contain the appropriate cysteine mutations were transformed into *E. coli* BL21(DE3) competent cells. Then expression,[3] purification,[3] and MTSSL labeling[1] of iso-1-cyt *c* were carried out. We estimated the overall spin label concentration by double integration of our spin labeled samples and comparison to a TEMPO standard and the protein concentration from the heme absorbance at 408 nm ($\epsilon_{408} = 1.08 \times 10^5$ M^{-1} cm^{-1}). From the combination of both estimates we determined that the efficiency of spin labeling of both sites was greater than 95%.

Characterization of the Bi-Labeled S47C−SL/K79C−SL. The labeling sites at S47 (Ser47) and K79 (Lys79) are external hydrophilic sites tolerant to mutation because both S47 and K79

are replaced by other nonconserved amino acids in functional homologous eukaryotic cytochromes.[40] The CD spectrum in the 210−250 nm region indicating helical content was identical from wild type (C102S), singly labeled S47C−SL and K79C−SL, and doubly labeled S47C−SL/K79C−SL. (Spin labeled variants are given the suffix "SL".) The thermal denaturation temperatures (T_m) for wild type, S47C−SL, K79C−SL, and S47C−SL/K79C−SL were respectively 53.6, 49.2, 47.8, and 44.6 °C. The S47C−SL/K79C−SL bi-labeled derivative definitely folded, and its 9 °C diminishment in melting temperature for the spin labeled double mutant was less than the sum of diminishments from the individual single mutations.

Results

We monitored the overall field-swept EPR line shape, where the integrated line shape, as opposed to the more standard first derivative line shape, is notably sensitive to dipolar broadening. This broadening is shown by the enhanced breadth of the outlying spectral wings and by a diminished depth of the valleys between peaks. We show in Figure 3A the absorbance spectrum (χ'') of folded bi-labeled S47C−SL/K79C−SL (solid) obtained under equilibrium conditions, and in Figure 3A, we compare this bi-labeled spectrum with the spectral sum from equal concentrations of singly labeled S47C−SL and K79C−SL (dotted). (Note: all labeling was >95% efficient.) The spectrum of folded bi-labeled S47C−SL/K79C−SL is broadened both in its wings and in the valleys between peaks at ambient temperature as compared to the sum of the two relevant singly labeled spectra. The notable effect of broadening in the valleys is to make the ratio of a given peak to valley smaller from the bi-labeled species. On the other hand, the line shapes of the GdnHCl-unfolded double mutants (Figure 3B) are narrow and virtually identical to those of the unfolded single mutants. In Figure 3, parts A′ and B′, we show the more standard first-derivative EPR spectra respectively corresponding to the absorbance spectra of Figure 3, parts A and B. The information content of both types of spectra is the same; however, derivative spectra enhance the sharp peak features as opposed to the wings and inter-peak valleys. The peak features are sharper from unfolded protein, as opposed to folded protein and from singly labeled folded protein, as opposed to folded bi-labeled protein.

Guanidinium-unfolded K79C−SL/S47C−SL was mixed with refolding buffer to a 0.66 M concentration of GdnHCl where the protein refolded. The accompanying Figure 4 compares the spectra of unfolded bi-labeled protein, bi-labeled protein refolded in 0.66 M GdnHCl, and most notably, spectra taken at 380 μs (Figure 4A), 1.2 ms (Figure 4B), and 1 s (Figure 4C) after the start of folding. It is evident that the dipolar broadened wings and general spectral breadth have only begun to set in by 1.2 ms after the start of folding. There is substantial evidence within 1 s of the start of folding from broadened wings and shallower valleys between peaks. A comparison may be made in the change to the depth of the valley between the first and second peaks in Figure 4A−C, where the unfolded and refolded valley depths provide end points. At 380 μs, 1.2 ms, and 1 s, the percentage increases from the unfolded to the completely folded depths were respectively 15, 25, and 65%.

In Figure 4A′−C′, we show the more standard first-derivative EPR spectra in which the derivative presentation tends to accentuate rapidly changing sharp peak features. From the derivative spectra it is especially obvious that the change in the sharp peak features has already occurred with 380 μs of the start of folding.

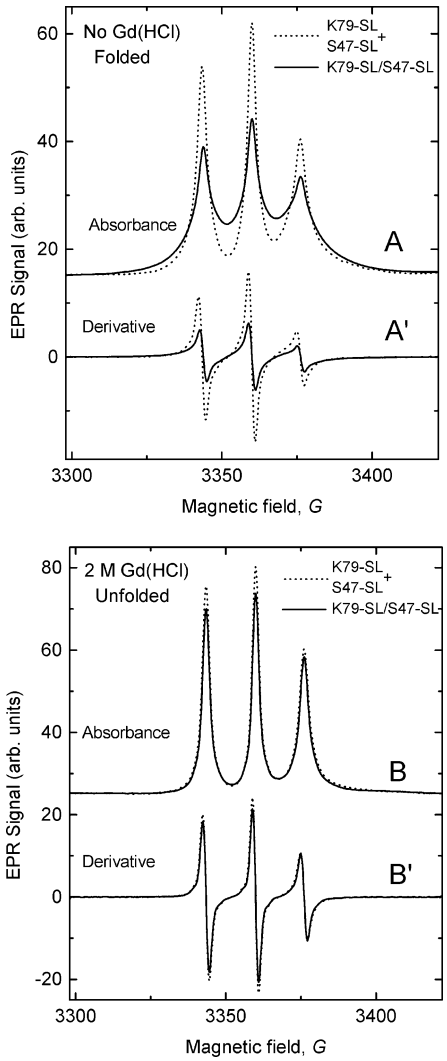

Figure 3. These figures were obtained under equilibrium conditions by CW EPR as carried out in a dielectric resonator on ~1 μL sample. The temperature was 22 °C. The absorbance (χ") EPR (part A) and corresponding first derivative (dχ"/dH) EPR (part A′) were obtained in dilute pH 5-folding buffer. Parts B (absorbance) and B′ (first derivative) were obtained with denaturing 2 M guanidinium chloride. The spectra of the K79C−SL/S47C−SL bi-labeled double mutant (solid line −) are compared in each of these figures with summed spectra from equal concentrations of the corresponding mono-mutants K79C−SL + S47C−SL (dotted line ···).

Discussion

The broadening shown under equilibrium folded conditions in the EPR spectrum of the folded S47C−SL/K79C−SL double mutant (Figure 3A) is typical of dipolar ($1/T_2$) line broadening arising from spin−spin dipolar interaction partially averaged by molecular tumbling.[30] The $1/T_2$ line broadening is inversely proportional to the sixth power of the interprobe distance R^{-6} and proportional to the tumbling correlation time of the protein.[30,41] By application of a spectral convolution scheme developed by Mchaourab and co-workers,[30] the distance between probe on S47C−SL and on K79C−SL from Lorentzian R^{-6} broadening was estimated at ~14 Å.[42] The difference between the spectra of folded bi-labeled folded protein and the sum of singly labeled folded protein (in both A and A′ of Figure 3) reflects the extra broadening due to spin−spin dipolar interaction for the bi-labeled protein. For proteins having labeling sites closer than those on S47 and K79 or proteins tumbling more slowly than cytochrome *c*, one might expect even more

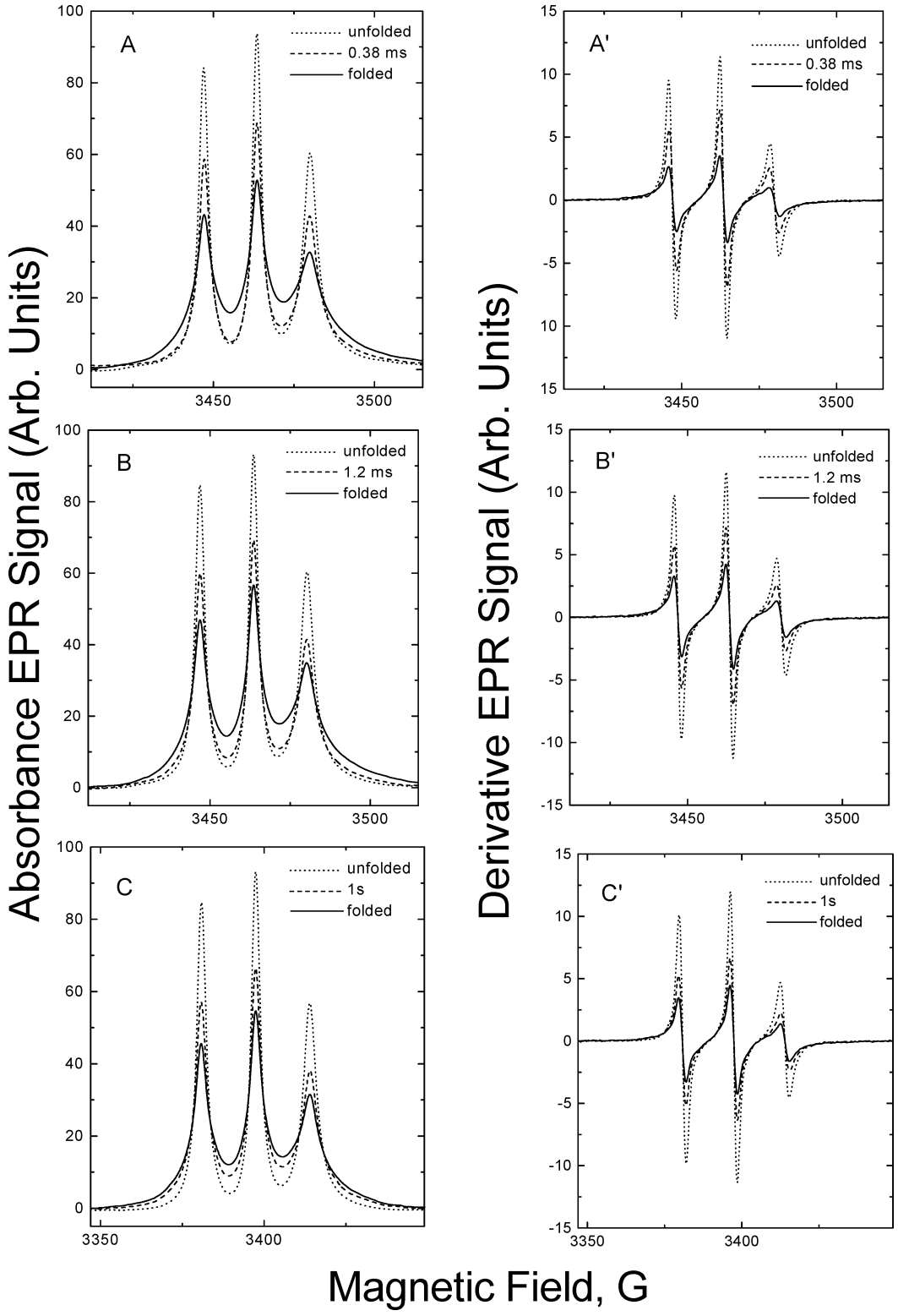

Figure 4. Comparison of rapid scanned spectra of bi-labeled S47C−SL/K79C−SL. The purpose of these figures is to compare unfolded bi-labeled protein (dotted line ···), folded bi-labeled protein (solid line —**)**, and partially folded spectra (dashed line ---) taken at 380 μs (A and A′), 1.2 ms (B and B′), and 1 s (C and C′) after the start of folding. Parts A, B, and C are absorption (χ'') presentations, whereas parts A′, B′, and C′ are the first derivative dχ''/dH presentations. Protein was denatured in 2.0 M GdnHCl, pH 5.0. Refolding was induced by a rapid 1:2 mixing of denatured protein in 2.0 M GdnHCl with dilute 0.05 M NaAcetate pH 5.0 buffer to give a 0.66 M GdnHCl denaturant concentration at which the protein folded. The final concentration of protein was close to 400 μM. The spectra A and A′ and B and B′ were obtained by flow EPR at flow rates calibrated to provide delivery times of 380 μs and 1.2 ms from ball-mixer to the center of the EPR active zone with a rapid scan time of 50 ms, a modulation of 1.6 G, and depending on flow rate, several seconds of data accumulation. Spectra C and C′ were obtained with a rapid scan of 50 ms triggered 1 s after stopped-flow and were the average of 75 such spectra.

spectrally evident broadening effects, both from folded protein and from folding protein, than those seen with cytochrome. The narrowness and sharpness of denatured protein EPR features (Figure 3, parts B and B′) as opposed to those of folded protein (Figure 3, parts A and A′) generally reflects the local greater mobility of the spin label in unfolded protein, and additionally

for the bi-labeled species, reflects the greater average distance between spin labels at positions 47 and 79 in unfolded protein.

The development of rapid-mixing combined with simultaneous rapid field scan has provided entire spectra of bi-labeled S47C−SL/K79C−SL protein caught in the act of folding from the submillisecond range to the second range. Absence of dipolar-broadening showed that folding had not sufficiently proceeded at 380 μs or at 1.2 ms to cause sequentially distant S47C−SL and K79C−SL spin labeled side chains to achieve their folded conformation, although diminishment of the immediate peak intensities did imply local probe enfolding and immobilization. These immediate peak intensities, shown to advantage in the derivative spectra of Figure 4, parts A′ and B′, are sensitive reporters of local probe immobilization which can occur in times shorter than 50 μs after the start of folding.[3] (For the future, a comprehensive set of rapidly scanned spectra of single mutants such as S47C−SL and K79C−SL will be provided to show the details of how single probes report local enfolding and immobilization.) For bi-labeled S47C−SL/K79C−SL iso-1-cyt-*c* folding also in the absence of imidazole, the rapid field scan triggered 1 s (Figure 4C) after the start of folding in the stopped-flow EPR mode showed where there was onset of dipolar-broadened features and proximity of the S47C−SL and K79C−SL side chains. As order prevailed, the spins on S47C−SL and K79C−SL drew near and the dipolar interaction became discernible. The evidence for dipolar interaction was most prominently shown by change in the depth of the valleys between peak features of the absorbance spectra.

Conclusion

It had not been experimentally clear for cytochrome when tertiary interactions between side chains set in, i.e., whether it was during the submillisecond prefolding or later during the major global > millisecond event marking cooperative, global folding. The time scale over which the interaction between distant side chains is established is significant to the nature of protein folding. Overall, our data empirically show from the diminishment of sharp peak intensity that rapid compacting occurs well within 380 μs of the start of protein folding and from the slow emergence of a dipolar interaction between spin labeled side chains that final establishment of tertiary interactions takes much longer. The new method reported here provides unique data on the dynamic onset of tertiary interaction between side chains never previously probed.

Acknowledgment. This work was supported by grants from the National Institutes of Health (GM066253-01A1) and the National Science Foundation (MCB-9817598).

References and Notes

(1) Qu, K.; Vaughn, J. L.; Sienkiewicz, A.; Scholes, C. P.; Fetrow, J. S. *Biochemistry* **1997**, *36*, 2884−2897.

(2) Grigoryants, V. M.; Veselov, A. V.; Scholes, C. P. *Biophys. J.* **2000**, *78*, 2702−2708.

(3) DeWeerd, K.; Grigoryants, V.; Sun, Y.; Fetrow, J. S.; Scholes, C. P. *Biochemistry* **2001**, *40*, 15846−15855.

(4) Nall, B. T.; Landers, T. A. *Biochemistry* **1981**, *20*, 5403−5411.

(5) Brems, D. N.; Stellwagen, E. *J. Biol. Chem.* **1983**, *258*, 3655−3660.

(6) Roder, H.; Elöve, G. A.; Englander, S. W. *Nature* **1988**, *335*, 700−704.

(7) Colon, W.; Elöve, G. A.; Wakem, L. P.; Sherman, F.; Roder, H. *Biochemistry* **1996**, *35*, 5538−5549.

(8) Elöve, G. A.; Bhuyan, A. K.; Roder, H. *Biochemistry* **1994**, *33*, 6925−6935.

(9) Colón, W.; Wakem, L. P.; Sherman, F.; Roder, H. *Biochemistry* **1997**, *36*, 6, 12535−12541.

(10) Creighton, T. E. *Nat. Struct. Biol.* **1994**, *1*, 135−138.

(11) Sosnick, T. R.; Shtilerman, M. D.; Mayne, L.; Englander, S. W. *Proc. Natl. Acad. Sci. U.S.A.* **1997**, *94*, 8545−8550.

(12) Akiyama, S.; Takahashi, S.; Ishimori, K.; Morishima, I. *Nat. Struct. Biol.* **2000**, *7*, 514−520.

(13) Pollack, L.; Tate, M. W.; Darnton, N. C.; Knight, J. B.; Gruner, S. M.; Eaton, W. A.; Austin, R. H. *Proc. Natl. Acad. Sci. U.S.A.* **1999**, *96*, 10115−10117.

(14) Shastry, M. C.; Roder, H. *Nat. Struct. Biol.* **1998**, *5*, 385−392.

(15) Lyubovitsky, J. G.; Gray, H. B.; Winkler, J. R. *J. Am. Chem. Soc.* **2002**, *124*, 5481−5488.

(16) Hagen, S. J.; Hofrichter, J.; Szabo, A.; Eaton, W. A. *Proc. Natl. Acad. Sci. U.S.A.* **1996**, *93*, 11615−11617.

(17) Telford, J. R.; Wittung-Stafshede, P.; Gray, H. B.; Winkler, J. R. *Acc. Chem. Res.* **1998**, *31*, 755−763.

(18) Telford, J. R.; Tezcan, F. A.; Gray, H. B.; Winkler, J. R. *Biochemistry* **1999**, *38*, 1944−1949.

(19) Hagen, S. J.; Eaton, W. A. *J. Mol. Biol.* **2000**, *297*, 781−789.

(20) Sienkiewicz, A.; Qu, K.; Scholes, C. P. *Rev. Sci. Instrum* **1994**, *65*, 68−74.

(21) Scholes, C. P. In *Biological Magnetic Resonance*; Eaton, G. R., Eaton, S. S., Berliner, L., Eds.; Kluwer: Norton, MA, 2004; Vol. 24, pp 53−87.

(22) Hubbell, W. L.; Altenbach, C. *Curr. Opin. Struct. Biol.* **1994**, *4*, 566−573.

(23) Mchaourab, H. S.; Lietzow, M. A.; Hideg, K.; Hubbell, W. L. *Biochemistry* **1996**, *35*, 7692−7704.

(24) Hubbell, W. L.; Gross, A.; Langen, R.; Lietzow, M. A. *Curr. Opin. Struct. Biol.* **1998**, *8*, 649−656.

(25) Miick, S. M.; Todd, A. P.; Millhauser, G. L. *Biochemistry* **1991**, *30*, 9498−9503.

(26) Marsh, D. In *Biological Magnetic Resonance*; Berliner, L., Ruben, J., Eds.; Plenum: New York, 1989; Vol. 8, pp 255−303.

(27) Schneider, D. J.; Freed, J. H. In *Biological Magnetic Resonance*; Berliner, L., Ruben, J., Eds.; Plenum: New York, 1989; Vol. 8, pp 1−76.

(28) Englander, S. W.; Sosnick, T. R.; Mayne, L. C.; Shtilerman, M.; Qi, P. X.; Bai, Y. *Acc. Chem. Res.* **1998**, *31*, 737−744.

(29) See Figure 5 and Table 2 of DeWeerd et al. (ref 3) for kinetic phases of folding in the presence of imidazole at pH 5 and their associated time constants and Figure S5A and Table S-5 in the Supporting Information of DeWeerd et al. for kinetic phases of folding in the absence of imidazole at pH 5 and their associated time constants. We note that some cytochromes *c*, including iso-1-cyt *c* spin labeled at naturally occurring C102 (ref 1), fold rapidly at pH 5 without exogenous imidazole (refs 5 and 8), although at pH 7 they show slower folding due to improper heme-histidine misligation.

(30) Mchaourab, H. S.; Oh, K. J.; Fang, C. J.; Hubbell, W. L. *Biochemistry* **1997**, *36*, 307−316.

(31) Borbat, P. P.; McHaourab, H. S.; Freed, J. H. *J. Am. Chem. Soc.* **2002**, *124*, 5304−5314.

(32) Louie, G. V.; Brayer, G. D. *J. Mol. Biol.* **1990**, *214*, 527−555.

(33) Banci, L.; Bertini, I.; Liu, G.; Lu, J.; Reddig, T.; Tang, W.; Wu, Y.; Yao, Y.; Zhu, D. *J. Biol. Inorg. Chem.* **2001**, *6*, 628−637.

(34) Pollock, W. B.; Rosell, F. I.; Twitchett, M. B.; Dumont, M. E.; Mauk, A. G. *Biochemistry* **1998**, *37*, 6124−6131.

(35) Morar, A. S.; Kakouras, D.; Young, G. B.; Boyd, J.; Pielak, G. J. *J. Biol. Inorg. Chem.* **1965**, *4*, 220−222.

(36) Kammann, M.; Laufs, J.; Schell, J.; Gronenborn, B. *Nucleic Acids Res.* **1989**, *17*, 5404.

(37) Landt, O.; Grunert, H. P.; Hahn, U. *Gene* **1990**, *96*, 125−128.

(38) Ke, S. H.; Madison, E. L. *Nucleic Acids Res.* **1997**, *25*, 3371−3372.

(39) Sarkar, G.; Sommer, S. S. *Nucleic Acids Res.* **1992**, *20*, 4937−4938.

(40) Moore, G. R.; Pettigrew, G. W. *Cytochromes c Evolutionary, Structural and Physicochemical Aspects*; Springer-Verlag: Berlin, 1990.

(41) Altenbach, C.; Oh, K. J.; Trabanino, R. J.; Hideg, K.; Hubbell, W. L. *Biochemistry* **2001**, *40*, 15471−15482.

(42) Following the scheme of Mchaourab and co-workers applied to bi-labeled T4 lysozyme (See formulas (1) and (2) of pp 313−314 of ref 30.), we used a Lorentzian broadening function in which the dipolar line broadening, ΔH_{dd}, was proportional to R^{-6} and proportional to the protein tumbling correlation time, τ_c. Since the molecular weight and volume of cytochrome are about two-thirds those of T4 lysozyme, a 4 nanosecond tumbling time was used for cytochrome rather than the 6 nanosecond tumbling time of the larger T4 lysozyme. (The peak width at half-height of the Lorentzian is $2\Delta H_{dd}$; the proportionality constant is approximately 5.5×10^{15} (Gauss) $Å^6\ s^{-1}$.) A Lorentzian function was numerically convoluted using Origin 7 with the sum of experimental single-mutant (S47C−SL + K79C−SL), field-swept spectra to simulate the bi-label spectrum of Figure 3A. From the value of $\Delta H_{dd} = 3 \pm 0.5$ G which best reproduced the bi-labeled spectrum, a value of R was extracted. That value of R was 14 ± 1 Å.